A Substrate-Assisted Concerted Mechanism for Aminoacylation by a Class II Aminoacyl-tRNA Synthetase†

Ethan Guth, Susan H. Connolly, Michael Bovee, and Christopher S. Francklyn*

Department of Biochemistry, University of Vermont, Health Sciences Complex, Burlington, Vermont 05405

Received September 24, 2004; Revised Manuscript Received December 14, 2004

ABSTRACT: Aminoacyl-tRNA synthetases (aaRS) join amino acids to their cognate transfer RNAs, establishing an essential coding relationship in translation. To investigate the mechanism of aminoacyl transfer in class II *Escherichia coli* histidyl-tRNA synthetase (HisRS), we devised a rapid quench assay. Under single turnover conditions with limiting tRNA, aminoacyl transfer proceeds at 18.8 s^{-1}, whereas in the steady state, the overall rate of aminoacylation is limited by amino acid activation to a rate of 3 s^{-1}. In vivo, this mechanism may serve to allow the size of amino acid pools and energy charge to control the rate of aminoacylation and thus protein synthesis. Aminoacyl transfer experiments using HisRS active site mutants and phosphorothioate-substituted adenylate showed that substitution of the nonbridging Sp oxygen of the adenylate decreased the transfer rate at least 10 000-fold, providing direct experimental evidence for the role of this group as a general base for the reaction. Other kinetic experiments revealed that the rate of aminoacyl transfer is independent of the interaction between the carboxyamide group of Gln127 and the α-carboxylate carbon, arguing against the formation of a tetrahedral intermediate during the aminoacyl transfer. These experiments support a substrate-assisted concerted mechanism for HisRS, a feature that may generalize to other aaRS, as well as the peptidyl transferase center.

The formation of aminoacyl-tRNA for protein synthesis occurs in two steps, the first of which entails activation of the amino acid to form a high energy anhydride aminoacyl−adenylate, followed by a transfer step in which the amino acid is attached to the 3′ terminal adenosine of the cognate tRNA. Accurate selection of cognate amino acid and tRNA by aminoacyl-tRNA synthetases (aaRS)[1] during this reaction is an important contributor to the fidelity of translation (*1*). The aaRSs can be divided into two classes of enzymes (*2*−*4*), each of which is organized around its own unique catalytic domain fold, enforces a different conformation of bound ATP, and exhibits distinct regiospecificity with respect to the use of the 2′ or 3′ OH of A76 during aminoacyl transfer (*5*). The mechanistic basis of aminoacylation, as well as the specific contributions of enzyme and substrate, is still a matter of active investigation.

Early studies on the adenylation reaction showed that aaRS bring amino acid and ATP substrates into reactive conformations, strengthening transition state binding to provide a significant rate enhancement (*6*−*9*). In contrast, the aminoacyl transfer half reaction is much less well-understood. Early studies focused on the molecular basis of tRNA recognition and indicated that noncognate tRNAs are rejected during steps that make a greater contribution to V_{max} than K_m (*10*). Other early work showed that tRNA binding involves multiple steps (*11*−*13*). However, the nature of the rate-determining step, and the role, if any, of a general base in facilitating aminoacyl transfer, remains to be determined. While initial studies on the class I isoleucyl enzyme suggested that release of the aminoacylated tRNA is the rate-determining step (*14*, *15*), Fersht and colleagues argued in subsequent work that aminoacyl transfer is rate limiting (*16*). In contrast, work on the representative class II seryl- and phenylalanyl systems suggested that aminoacyl transfer and amino acid activation can both serve as rate-determining steps, depending on substrate conditions (*12*, *13*). With regard to the identification for a general base in the aminoacyl transfer reaction, a role for the nonbridging oxygens of the adenylate has been invoked but without any direct supporting experimental evidence (*17*, *18*).

With these questions in mind, we set out to address the mechanism of the aminoacyl transfer reaction, employing *Escherichia coli* histidyl-tRNA synthetase (HisRS) as a model system. HisRS is suitable for these studies because the enzyme is a small class II α_2 dimer that lacks the complex editing functions of other, larger aaRS (*19*). Crystal structures have been reported that comprise all of the individual steps of the adenylation reaction (*20*−*23*), and the molecular basis of tRNA recognition has been studied extensively (*24*−*28*). Here, we used a rapid chemical quench assay to isolate the aminoacyl transfer step and thereby determine the rate of transfer for wild-type HisRS, selected active site mutants, and phosphorothioate substituted adenylates. On the basis of these studies, we show that the rate of aminoacyl transfer

† This work was supported by the Grant GM54899 from the National Institutes of Health.

* Correspondence should be addressed to the following author. E-mail: franck@emba.uvm.edu. Phone: (802) 656-8450. Fax: (802) 862-8229.

[1] Abbreviations: aaRS, aminoacyl-tRNA synthetase; ATPαS , adenosine thiotriphosphate; DTT, dithiolthreitol; HEPES, *N*-(2-hydroxyethyl)piperazine-*N*′-(2-ethanesulfonic acid); K_d, dissociation constant; k_{obs}, observed rate constant; $MgCl_2$, magnesium chloride; PEI, polyethyleneimine; KCl, potassium chloride; NaOAc, sodium acetate; TLC, thin-layer chromatography; TEAB, triethylammonium bicarbonate; TCA, trichloroacetic acid.

10.1021/bi047923h CCC: $30.25
Published on Web 02/18/2005

is faster than the steady-state rate of aminoacylation, which appears to be limited by the rate of amino acid activation. Furthermore, the aminoacylation reaction is shown to be substrate assisted and concerted, features that can readily be identified in other aaRS systems.

EXPERIMENTAL PROCEDURES

General Chemicals and Reagents. Unless otherwise noted, chemicals were provided by Fisher Scientific and Sigma. Most restriction endonucleases and enzymes for molecular biology were supplied by New England Biolabs. The oligonucleotides for site-directed mutagenesis were obtained from Operon Technologies. The restriction endonuclease EcoT22I was purchased from Amersham, as was the L-[2,5 ^{3}H] histidine. The specific activity of the latter was typically 40−70 Ci/mmol. The Protein Quick Spin columns and ATPαS (Sp isomer) were purchased from Roche. ADPαS (Rp isomer) was a gift from Fritz Eckstein. The Ni−NTA agarose was purchased from QIAGEN. All reagent solutions were prepared in filtered milliQ water.

Synthesis of ATPαS (Rp). The protocol for synthesis of the ATPαS Rp stereoisomer has been described previously (*29*). The ADPαS Rp isomer was obtained from Fritz Eckstein as the TEAB salt. The material was washed twice with 1.0 mL aliquots of methanol and then evaporated to dryness in a Speed-Vac. In a typical phosphorylation reaction, 0.4 μmol of ADPαS (Rp) was resuspended in 15 mM Tris-HCl (pH 8.9), 0.75 mM DTT, 1.5 mM $MgCl_2$, and 4.5 mM creatine phosphate. The reaction was initiated by the addition of 20 U of creatine kinase and then allowed to proceed for 3 h at room temp. The progress of the conversion of ADP to ATP was monitored by thin-layer chromatography (TLC) on PEI-cellulose, employing 0.75 M KH_2PO_4 as the mobile phase. Although ∼50% of the ADP appeared to be hydrolyzed to AMP, the majority of ADP was converted within 3 h. ATP was purified from the resultant mixture by DEAE chromatography. AMP, ADP, and ATP were eluted sequentially from the DEAE column in a linear gradient of 0.1−0.6 M TEAB. The identity of the eluted nucleotides was confirmed by thin-layer chromatography; the fractions containing ATP were essentially homogeneous. Pooled fractions containing ATP were evaporated to dryness and washed three times in methanol as stated previously. ATPαS (Rp) was reconstituted in ddH_2O, the pH was adjusted to 7.0 with NaOH, and then its concentration was determined by absorbance at 260 nm, using a molar extinction coefficient of 15 500 M^{-1} cm^{-1}.

Preparation of Aminoacyl- tRNA Synthetases and tRNA. The wild-type and mutant HisRSs were produced from expression strains containing derivatives of pWY-1, a HisRS expression plasmid featuring the strong T6 promoter and a *lac* operator to permit induction by IPTG (*25*). The E83A, E83Q, and Q127A mutations were introduced into pWY-1 by use of the Quick Change protocol (Stratagene), as described previously (*27*). Mutagenic primers were 33−36 nucleotides in length and were designed to obtain target melting temperatures of 72−75 °C. The mutations were confirmed by DNA sequencing of *hisS*. The construction of the R259H mutant was described previously (*21*). To express wild-type and mutant proteins, late log cells were induced for 4 h by addition of IPTG to a final concentration of 0.5 mM. All HisRS proteins were purified by Ni−NTA affinity chromatography (*27*), making use of the His_6 affinity tag encoded by pWY-1 and its derivatives. An earlier study demonstrated that the presence of the His_6 tag does not significantly alter the catalytic properties of HisRS (*25*). Purified HisRS fractions from nickel affinity chromatography were pooled, concentrated, and dialyzed into storage buffer (50 mM Tris-HCl [pH 7.5], 100 mM KCl, 5 mM β-mercaptoethanol, 45% glycerol). The resulting preparations were greater than 95% pure, and the concentration of HisRS was determined from its absorbance at 280 nm, using an extinction coefficient of 127 097 M^{-1} cm^{-1} (*25*). Transcripts of the wild-type $tRNA^{His}$ were produced by in vitro transcription, using T7 RNA polymerase. Two different plasmid constructs were used for production of templates. The initial quench flow studies utilized templates produced by EcoT221 digestion of plasmid pWY-40 (*25*). This restriction enzyme generates a 3′ overhang that must be filled in by use of the Klenow fragment of DNA Pol I and dNTPs. To obviate the need for this additional step, a new plasmid was constructed with a FokI site located at the 3′ end of tRNA gene. The procedures employed for in vitro transcription reactions and purification of transcripts scheme have been described previously (*27*).

Steady-State Kinetics of Pyrophosphate Exchange and Aminoacylation. The steady-state kinetic parameters of pyrophosphate exchange for the wild-type and mutant enzymes were determined by retention of radiolabeled ATP on activated carbon, as described previously (*27*, *28*, *30*). The in vitro aminoacylation assays were carried out using methods published previously (*25*, *27*). The concentrations of active tRNA from the transcript preparations were determined from the plateau values of aminoacylation and were typically at least 50% of the theoretical maximum based on absorbance. Aminoacylation reactions were incubated at 37 °C and pH 7.5, with the duration of the time courses dependent on the activity of the mutant, and chosen to emphasize the linear phase of product formation. Kinetic parameters were determined from plots featuring at least five different tRNA concentrations, generally spanning 0.2−5 times K_m. The data were fit to the Michaelis−Menten equation using the KaleidaGraph software package (Synergy software, version 3.08d)

Pre-Steady-State and Single Turnover Kinetics. The general approaches for these assays were described in work by Fersht and co-workers (*16*, *31*). As a prelude to rapid kinetic assays, large quantities of the HisRS histidyl−adenylate complex were prepared as follows. A typical 300 μL reaction contained HisRS at a final concentration of 30 μM, in the presence of 2.5 mM ATP and 60 μM [^{3}H]-histidine, incubated in a standard adenylation reaction buffer (10 mM HEPES [pH 7.5], 100 mM KCl, 1 mM DTT, and 10 mM $MgCl_2$). The inclusion of 0.2 U of yeast inorganic pyrophosphatase (PPi-ase) ensured that the adenylation reactions were effectively irreversible. Following a 30 min incubation, the enzyme bound adenylate complex was separated from unincorporated substrates by G25 spin column chromatography (Roche) using columns preequilibrated with adenylation reaction buffer. The isolated enzyme:adenylate complex was then stored on ice for immediate use in single turnover or pre-steady-state quench flow assays. For single turnover experiments, the spin column purified adenylate

complex was used in one syringe of the KinTek RQF-3 rapid quench apparatus, while the second syringe contained tRNA in adenylation reaction buffer. The reaction time courses were constructed by the reaction being sampled over a time interval of 0.01−5 s (representing ~10 half-lives) and being quenched with 3 M sodium acetate (pH 4.5). For slow mutants, aliquots of the reactions were removed by manual sampling over an interval that ranged from 10 to 120 min. To ensure dissociation of enzyme and substrates, the collection tubes contained SDS to a final concentration of 1%. Aminoacylated tRNA in reaction aliquots was precipitated on 5% TCA soaked Whatman filter pads according to the standard procedure (*27*). The amount of aminoacylated tRNA product was plotted versus time and fit to the first-order exponential equation

$$y = a + b(1 - \exp^{-kt})$$

where a = the y intercept, b = the scaling constant, k = the observed rate, and t = time in seconds.

For pre-steady-state reactions where the tRNA was in excess over the adenylate complex, one syringe contained HisRS and tRNA (2 μM HisRS, 20 μM $tRNA^{His}$, 10 mM HEPES [pH 7.5], 100 mM KCl, 1 mM DTT, and 24 mM $MgCl_2$), while the second contained 6 mM ATP, 200 μM [^{3}H]- histidine, 10 mM HEPES [pH 7.5], 100 mM KCl, 1 mM DTT, 24 mM $MgCl_2$, and 4 units/mL inorganic pyrophosphatase. Reaction aliquots of 20 μL were collected at time points from 10 ms to 30 s and then quenched as stated previously. The procedure was repeated by [α-^{32}P] ATP being substituted as the radiolabeled substrate, and [α-^{32}P] AMP production being monitored by PEI-cellulose TLC with 0.75 M K_2PO_4 as the mobile phase. To improve the sensitivity, enzyme and tRNA concentrations in the first syringe were raised to 5 and 50 μM, respectively, while the concentration of ATP in the second syringe was decreased to 100 μM. In both syringes, the $MgCl_2$ concentration was lowered to maintain a 4:1 ratio with ATP. TLC plates were developed on a Bio-Rad imaging screen K and scanned using a Bio-Rad FX molecular imaging system. The Quantity One software package (Bio-Rad, Hercules, CA) was used to analyze the resulting images.

RESULTS

Single Turnover Rate of Aminoacyl Transfer Is Faster than the Steady-State Rate of Aminoacylation. To determine the rate of aminoacyl transfer, we employed the rapid chemical quench method (*32*). To achieve single turnover conditions, histidyl−adenylate was preformed on the enzyme in the presence of pyrophosphatase and then separated from unreacted substrates by size exclusion chromatography. A quantification of the ratio of preformed adenylate to HisRS enzyme by scintillation counting showed a consistent stoichiometry of one adenylate molecule bound per dimer (data not shown). The titration of a fixed concentration of preformed HisRS adenylate (1 μM) with $tRNA^{His}$ (0.2−5 μM) produced progress curves that readily fit to a single exponential equation and indicated that >75% of adenylate is chemically competent for transfer (data not shown). When excess enzyme:adenylate complex and tRNA were rapidly mixed, the resulting first-order progress curves were fit to a single exponential with a k_{obs} of 18.8 s^{-1} (Figure 1A). This rate is at least 6-fold higher than the steady-state rate of histidylation, previously determined to be 2.5 s^{-1} (*27*). The amplitude of tRNA charged in some pre-steady-state experiments was less than the theoretical maximum predicted based on aminoacylation plateaus, reflecting either sequestration of competent tRNA by nonadenylated active sites or a subpopulation of misfolded tRNA with a reduced rate of aminoacylation.

Is the Rate of Aminoacylation Limited by Product Release? The observed discrepancy between single turnover and steady-state rates of aminoacylation could reflect a rate-determining step after aminoacyl transfer, such as the release of aminoacylated tRNA from the enzyme. To further distinguish between the actual transfer step and the product release step, a preformed HisRS−$tRNA^{His}$ complex (at a 10:1 tRNA:enzyme ratio) was mixed with ATP and [^{3}H]-histidine under pre-steady-state conditions (*16*, *32*). Under these conditions, the observation of burst kinetics would indicate that release of product occurs more slowly than the actual transfer step; if transfer is slower, then the pre-steady-state rate should approximate the steady-state rate. As shown in Figure 1B, however, the steady-state rate (3.14 s^{-1}) was reached during the first turnover of the enzyme, with no apparent break in the curve. This experiment was extended from the pre-steady state through five turnovers, with no decrease in the rate of product production. Hence, product release is not rate limiting for aminoacylation and thus cannot account for the discrepancy between the rate of aminoacyl transfer and the overall rate of aminoacylation measured by steady-state kinetics.

HisRS-catalyzed pyrophosphate exchange occurs at a rate of 120 s^{-1} (*30*), suggesting that the isolated half reactions of adenylate formation and aminoacyl transfer are both faster than the overall steady-state rate of aminoacylation. With product release eliminated as a limiting step for the overall rate of aminoacylation, we considered the possibility that the rate of the adenylation reaction is influenced by the presence of excess tRNA. To address this possibility, additional HisRS pre-steady-state experiments were conducted to monitor the adenylation process. In these experiments, conversion of [α-^{32}P] ATP to AMP−adenylate was followed by thin-layer chromatography (TLC). As seen in experiments monitoring the production of aminoacylated tRNA under pre-steady-state conditions (Figure 1B), a linear accumulation of AMP in the first and successive turnovers was observed when tRNA was present in the reaction, and no evidence for a burst was observed in the first turnover relative to those that followed (filled circles, Figure 1C). Parallel experiments monitoring the production of PPi gave essentially the same result (data not shown). When tRNA was omitted from the reaction, the initial rate of AMP formation was faster than the reaction containing tRNA, and the production slowed dramatically at a stoichiometry of approximately one adenylate formed per dimer (open circles, Figure 1C). These experiments provide direct evidence that, in the histidine system, the presence of tRNA reduces the rate of adenylation below that of the tRNA-independent reaction. However, the tRNA clearly facilitates multiple turnovers in the adenylation reaction, providing a clear illustration of how the two processes are coupled. Without tRNA in the reaction, the adenylation reaction catalyzed by HisRS may be limited by the dissociation constants for

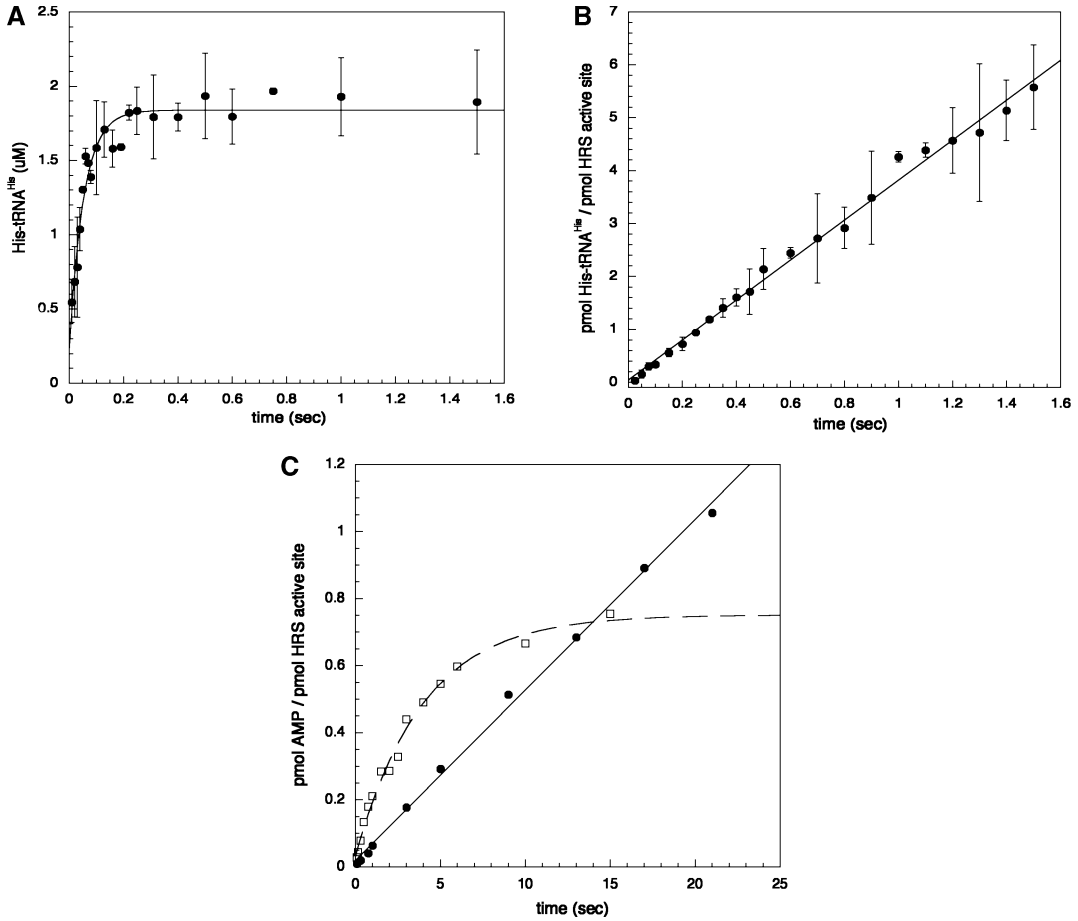

FIGURE 1: Aminoacyl transfer at 37 °C, pH 7.5, under single turnover and pre-steady-state conditions. (A) Single turnover assay at 37 °C, pH 7.5, for aminoacyl transfer catalyzed by HisRS. The wild type enzyme:adenylate complex was produced as described in Experimental Procedures and then rapidly mixed with $tRNA^{His}$ (8 μM) in the quench flow apparatus. (B) Product release is not rate limiting under pre-steady-state conditions. HRS (2 μM) and $tRNA^{His}$ (20 μM) were rapidly mixed with equal volumes of ATP (6 mM), [2,5-^{3}H] histidine (200 μM), and PPiase (4 U/mL). Reactions were terminated with 3 M NaOAc. Data were collected to at least 1.5 s, which is >6.5 half-lives. (C) Pre-steady-state time course of aminoacylation, monitoring the production of [α-^{32}P] AMP. The reaction conditions were as described above (B) save for an increase in HRS (5 μM) and tRNA (50 μM) and a decrease in ATP (100 μM). The assay was performed with tRNA (closed circles) and without (open squares). The data without tRNA, representing a single turnover of adenylate production, is fit to a single exponential.

histidine, ATP, or His∼AMP adenylate and thus display apparent single turnover kinetics. Nonetheless, the initial portions of both traces describe the adenylation reaction prior to aminoacylation and are thus comparable.

Mutations in Histidyl−tRNA Synthetase Differentially Affect Single Turnover and Steady-State Rates. The active site of the HisRS histidyl−adenylate complex can be readily superimposed on those of the ThrRS:$tRNA^{Thr}$ and AspRS:$tRNA^{Asp}$ complexes (*33*, *34*), providing a basis for modeling the position of A76 (Figure 2). Previously, we used this model to derive predictions about contacts between the *E. coli* HisRS and the CCA end of the cognate tRNA and then tested these by mutagenesis and kinetic analysis (*27*, *28*). This docking model indicates that residues important for aminoacyl transfer likely include Arg259, which interacts with the Sp nonbridging oxygen of the adenylate; Arg113, which interacts with the Rp nonbridging oxygen; Gln127, which contacts the α-carbonyl of the adenylate; and Glu83, which interacts with the α-amino group. The position of Glu83 would also allow it to fix the position of the terminal A76 in the reaction via a hydrogen bond to the 2′OH, or alternatively, serve as a general base by abstracting a proton from the 3′OH.

The contributions of these individual contacts (save for Arg113) were assessed by mutagenesis, followed by steady-state and pre-steady state kinetics analysis. Steady-state kinetic data for R259H HisRS were reported previously (*21*) and showed that pyrophosphate exchange and aminoacylation are reduced by factors of 1000- and 3000-fold, respectively (Table 1). Notably, the overall steady-state rate of R259H pyrophosphate exchange was only 2-fold greater than the rate of aminoacylation. An even greater decrease (4500-fold) in steady-state aminoacylation kinetics was observed for E83A HisRS. This decrease was partially, but not entirely, rescued by the E83Q mutation. In contrast to the R259H and E83A substitutions, the Q127A substitution caused a much smaller effect, decreasing pyrophosphate exchange 54-fold and aminoacylation 70-fold. Q127A was also seen to provide a 40-fold increase in K_m for histidine. Thus, loss of contacts to charged groups on the adenylate (i.e., the α-NH_3 and -phosphate) were associated with much greater decreases in activity than contacts to the uncharged α-carbonyl.

To more precisely assess the role of these side chains in the aminoacyl transfer step, product formation rates for these mutants were measured in single turnover quench experiments. Although reduced adenylation efficiency in the

Table 1: Steady-State Rates of Pyrophosphate Exchange and Aminoacylation along with Single Turnover Rates of Aminoacylation of HisRS Mutants

	steady state					single turnover
	pyrophosphate exchange			aminoacylation		aminoacylation
	K_m (μM) histidine	K_m (μM) ATP	k_{cat} (s^{-1})	K_m (μM) $tRNA^{His}$	k_{cat} (s^{-1})	k_{trans} (s^{-1})
WT	30 ± 5	890 ± 64	130 ± 5	0.34	2.02	18.8 ± 2.5
R259H[a]	25 ± 5	370 ± 12	0.103 ± 0.010	3.30	0.006	0.0066 ± 0.00031
E83A	134 ± 18	N.D.[b]	0.201 ± 0.001	5.15	0.004	0.0026 ± 0.00011
E83Q	35.3 ± 4.4	N.D.[b]	0.329 ± 0.010	0.17	0.01	0.0055 ± 0.00053
Q127A	996 ± 131	N.D.[b]	2.2 ± 0.083	0.48	0.048	9.2 ± 1.1

[a] Steady-state kinetic data for R259H were published in ref *21*. [b] Not determined. Steady-state and single turnover measurements were carried out at 37 °C, as described in Experimental Procedures. At least three independent experiments were averaged to give the values. Standard deviations for replicate experiments were within 10%. For steady-state measurements on mutant enzymes, 100 nM enzyme concentrations and extended time courses were employed.

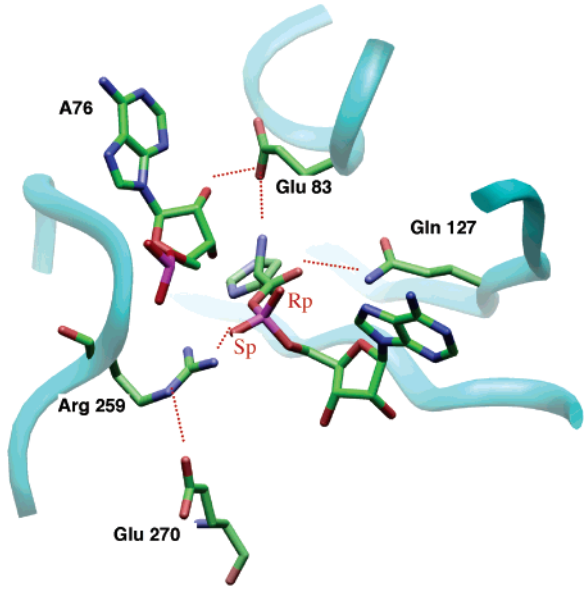

FIGURE 2: Active site of the HisRS−histidyl adenylate complex (PDB ID: 1KMM) with the position of A76 modeled in. Secondary structures that make up the histidine binding loop and β-strands that comprise the floor of the class II active site are depicted as cyan colored ribbons. Selected active site side chains and the bound adenylate are stick rendered in CPK coloring. The position of A76 (also in CPK coloring) was modeled based on superposition of HRS with the ThrRS (PDB ID: 1COA) and *E. coli* AspRS (PDB ID: 1QF6) complexes with cognate tRNA. During the course of the formation of the adenylation reaction, the α-phosphate undergoes stereochemical inversion, such that ATPαS (Sp) gives rise to sulfur in the Rp nonbridging oxygen, and ATPαS (Rp) gives rise to sulfur in the Sp position.

mutants did lead to a decrease in the formation of stable enzyme adenylate that could be isolated (yields of 5, 8, 40, and 50% were obtained for E83A, E83Q, R259H, and Q127A HisRS, respectively, relative to the wild-type enzyme), first-order progress curves were observed in all cases. Manual sampling of product formation catalyzed by R259H, E83A, and E83Q HRS mutants provided fitted rates of 0.005, 0.007, and 0.01 s^{-1} (Figure 3A−C), respectively, which were in close agreement with the steady-state rates. As in the case of the steady-state kinetics, the deleterious effects of E83A were not significantly rescued by E83Q. Thus, mutations at Glu83 and Arg259 limited both pre-steady-state and single turnover aminoacylation to a maximum rate of ~0.005 s^{-1}, which was at least 17-fold slower than the rate of pyrophosphate exchange (Table 1). In contrast, Q127A HisRS exhibited a rate of transfer that was only 2-fold less than the single turnover rate of aminoacyl transfer by wild-type HisRS (9 vs 18 s^{-1}) but considerably faster than the steady-state rate of either pyrophosphate exchange (2.2 s^{-1}) or aminoacylation (0.048 s^{-1}). The preferential effect of the Q127A mutation on the adenylation reaction was therefore unique to this mutant protein and suggests that the contact between Gln127 and α-carbonyl is not important for the transition state for aminoacyl transfer.

Aminoacyl Transfer with Phosphorothioate Substituted Adenylates. Single turnover aminoacyl transfer and steady-state aminoacylation are therefore limited at different steps, a difference that was uncoupled by some but not all of the active site mutants. To gain further insight into the nature of the chemical step for aminoacyl transfer, the effect of modifying leaving group chemistry was investigated. Histidyl−adenylate complexes using both ATPαS (Sp) and ATPαS (Rp) were assembled on the wild-type, R259H, and E83A HisRS enzymes, and then the rates of single turnover transfer to $tRNA^{His}$ were determined in the quench apparatus or by manual sampling. Despite differences in the relationship of single turnover to steady state, as well as differences in absolute rates, wild-type, R259H, and E83A HisRS all exhibited identical stereochemical preferences with respect to the two adenylate diastereomers (Figure 4A,B, summarized in Table 2). In each case, the rates of aminoacyl transfer of the Rp adenylates were only 15−30-fold slower than the all-oxygen adenylates. While the rates of turnover of the Sp adenylates could not be reliably fitted as first order exponentials, an analysis of initial rates of transfer indicated that, for the wild-type enzyme, the oxygen to Rp thio-substitution reduced the rate 50-fold, while the Sp thio-substitution reduced the rate at least 10 000-fold. In comparison, 17- and 400-fold reductions were observed for the R259H enzyme using the Rp and Sp diastereomers, respectively. The magnitude of this thio effect suggests that the rate of aminoacyl transfer is limited by the rate of aminoacyl transfer chemistry and is consistent with the involvement of the nonbridging Sp oxygen in that chemistry.

DISCUSSION

Overall Rate of Aminoacylation Is Limited by the Rate of Adenylate Formation. A surprising conclusion from our study is that the overall rate of aminoacylation (k_{cat}) is slower than the individual rates of either amino acid activation or aminoacyl transfer. The rate of 18.8 s^{-1} measured in our single turnover experiments likely reflects the rate of aminoacyl transfer chemistry, both because no lag or multiple

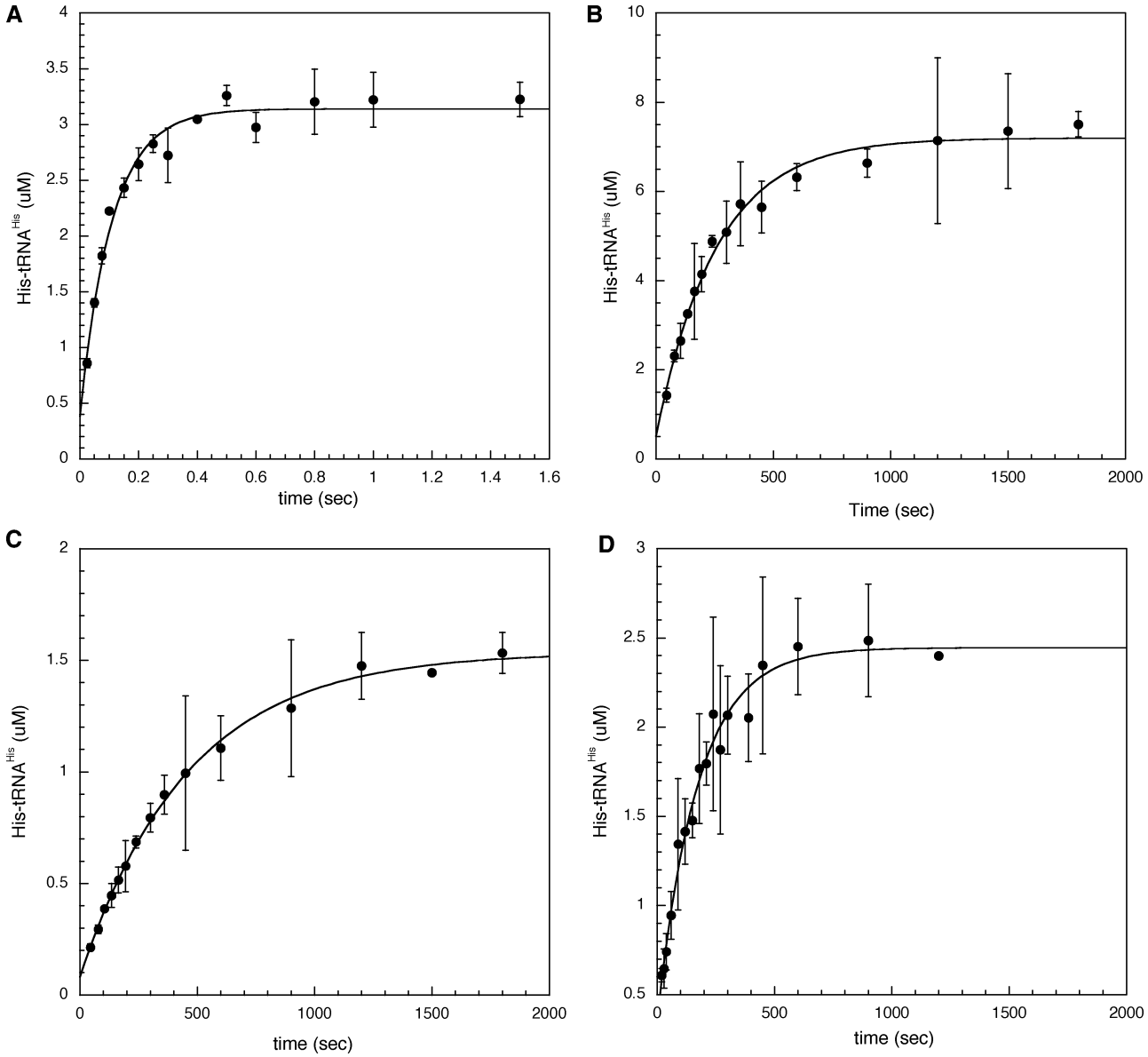

FIGURE 3: Single turnover progress curves for aminoacyl transfer catalyzed by HisRS active site mutants at 37 °C, pH 7.5. Q127A (A), R259H (B), E83A (C), and E83Q (D). Enzyme:adenylates were preformed, isolated, and rapidly mixed with tRNA^{His} (8 μM) as described in the legend for Figure 1. Reaction times smaller than 5 s were carried out in the rapid quench apparatus, while longer time-points were obtained by manual sampling, terminating the reaction by being spotted onto TCA saturated filters.

exponentials were seen (indicating that tRNA binding is not limiting) and because a previous rate versus pH profile argues against a rate-limiting conformational change (*35*). The phosphorothioate substitution experiments are also consistent with chemistry being rate limiting. The overall rate of aminoacylation cannot be limited by the rate of product release because no burst of aminoacylated tRNA was observed under pre-steady-state conditions (Figure 1B). When the production of aminoacylated tRNA and the production of adenylate were monitored in parallel, no burst of adenylate production accompanied production of the first equivalent of tRNA (Figure 1C), and tRNA explicitly depressed the rate of adenylate formation (Figure 1C). The simplest explanation for these observations is that presence of the tRNA limits the rate of amino acid activation, a conclusion also drawn from a previous study of the yeast seryl-tRNA synthetase system (*36*). Early work in the SerRS and PheRS systems also suggested that adenylate formation is rate limiting in the presence of tRNA, much as we have proposed here (*12*, *13*, *37*). A survey of more recent literature indicates that faster rates of aminoacyl transfer relative to the steady-state k_{cat} are characteristic of all the dimeric class I and II enzymes for which detailed pre-steady-state kinetic measurements have been reported (Table 3). While a rate-limiting step involving release of aminoacylated product can account for the overall slower rate of k_{cat} in class I systems (*38*, *39*), the same cannot be said of class II enzymes. Previously, Fersht et al. rationalized the discrepancy between pre-steady-state and steady-state kinetics on the basis of subsaturating substrate concentrations and site−site interactions (*40*). Neither of these explanations can account for the behavior observed with HisRS as the pre-steady-state experiments in Figure 1B were carried out with saturating substrates, and HisRS does not exhibit classical half-of-sites behavior in reactions where tRNA is present.

Mechanisms in which the overall rate of aminoacylation is limited by amino acid activation have important implications for the regulation of the rate of protein synthesis by

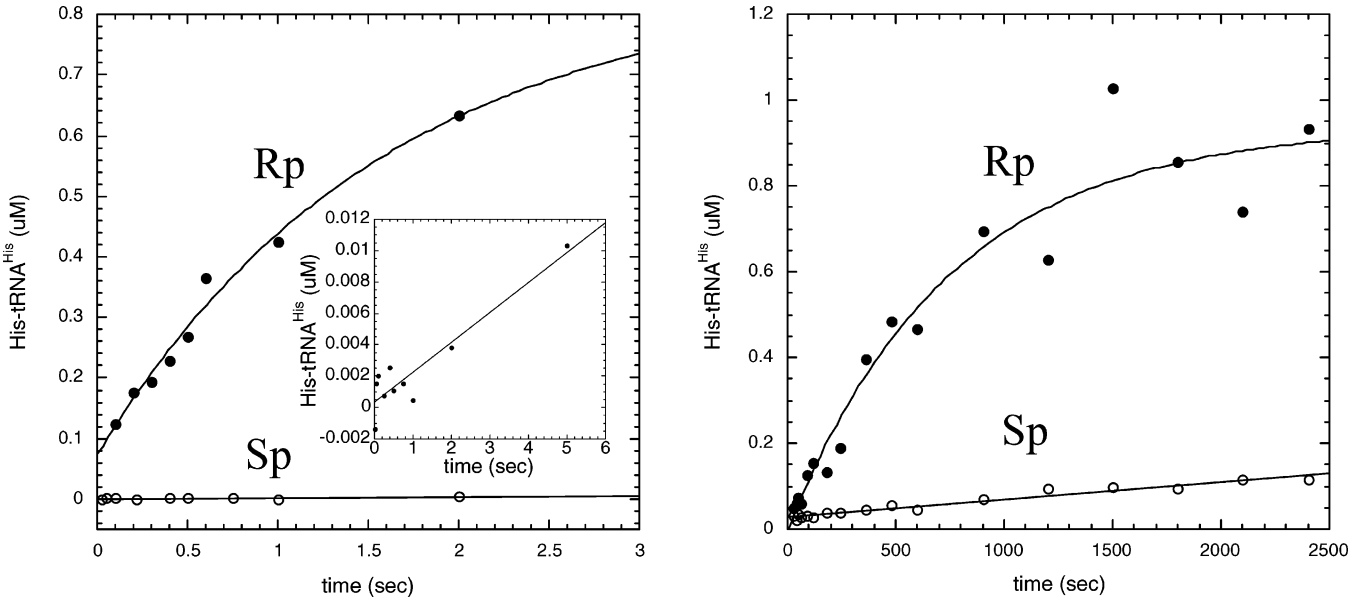

FIGURE 4: Aminoacylation stereospecificity of thio-substituted histidyl-adenylates. Aminoacyl transfer catalyzed by wild-type HisRS (A) and R259H HisRS (B), using Rp and Sp phosphorothioate substituted histidyl−adenylates. Wild-type or mutant enzyme (30 μM) was preincubated with [^{3}H] histidine, ATPαS (Rp or Sp isomer), and PPi-ase for 1 h at 25 °C. Enzyme−adenylate complexes were then isolated and rapidly mixed with tRNA^{His} (8 μM) before the reaction was terminated by being quenched with 3 M NaOAc (rapid quench flow apparatus) or by being spotted on 5% TCA soaked filter paper (manual sampling). For the Rp diastereomer, the solid lines represent the best fit to a single exponential equation. Sp isomer data could not be reliably fitted to a single exponential and instead were fitted to a straight line by linear regression. Inset shows wild-type enzyme with Sp thioisomer at later time points.

Table 2: Stereochemical Effect of Phosphorothioate Adenylate on Aminoacyl Transfer

	ATP	ATPαS Rp	ATPαS Sp	thio effect [O]/[S] Rp	thio effect[a] [O]/[S] Sp
WT	18.8 ± 2.5	0.63 ± 0.21	N.D.[b]	50.1	10000
E83A	0.0026 ± 0.0001	0.0011 ± 0.0001	N.D.[b]	2.4	200
R259H	0.0066 ± 0.0003	0.0011 ± 0.0003	N.D.[b]	6	400

[a] Based on estimates fitting to the initial linear portions of progress curves. [b] Not determined.

Table 3: Comparison of Rate Constants for Steady-State Aminoacylation (k_{cat}) and Pre-Steady-State/Single Turnover Aminoacyl Transfer (k_{trans}) in Different Class I and Class II aaRS Systems

AaRS system	k_{trans} (s^{-1})	k_{cat} (s^{-1})	method of pre-steady kinetic analysis	ref
Ec[a]HisRS	18.8	2.5	rapid quench	this paper
Bb[b]TyrRS	28−30	3.7	stop flow/quench	31
Bb[b]TrpRS	44	2.9	stop flow	56
Ec[a]SerRS	35	2.4	rapid quench	12
Sc[c]PheRS	35	2.4	stop flow	13

[a] *E. coli*. [b] *B. stearothermophilus*. [c] *S. cerevisiae*.

aminoacylation. Notably, the pre-steady-state experiments described in Figure 1B were performed at micromolar concentrations of aaRS with tRNA in excess, which reflect physiological concentrations and aaRS:tRNA ratios in vivo (*41*). Enzyme−tRNA ratios are constant under a wide variety of physiological conditions, where ratios of aaRS to ATP and to amino acid are likely to fluctuate on the basis of the size of individual amino acid pools and cellular energy charge. Notably, early work showed that HisRS activity is sensitive to the cellular energy charge (*42*). Thus, coupling the overall rate of aminoacylation to the rate of amino acid activation is logical because it allows aaRSs to provide a level of control over protein synthesis by serving as sensors of ATP levels and amino acid pools (*43*).

Substrate Assisted Catalysis and the Nature of the General Base for Aminoacyl Transfer. The aminoacylation reaction involves decomposition of a mixed anhydride (the aminoacyl adenylate) to form an aminoacyl ester, a thermodynamically favorable process. The rate of this reaction should nonetheless be enhanced by the action of a general base. By virtue of its position in the active site (Figure 5), the significant consequences of its substitution by alanine or glutamine, and the likely pK_a of its γ-oxygens (∼4−5), Glu83 would appear upon first inspection to be a good candidate for the general base. Yet Glu83 is also situated to neutralize the α-amino group of the substrate histidine (*20*, *21*), an interaction that would increase the nucleophillicity of histidine's α-carboxylate in the adenylation reaction, while also positioning the adenylate for the subsequent aminoacyl transfer reaction. The low levels of recoverable HisRS adenylate with both alanine and glutamine substitutions testify as to the importance of the salt bridge in binding and retaining the adenylate prior to transfer. This suggests that the dependence of the rate of the aminoacyl transfer reaction on Glu83 can be rationalized on the basis of electrostatic grounds (as opposed to a direct role as general base), which would also account for the observed conservative substitution of Glu83 by aspartate in eukaryotic versions of HisRS (*30*).

As there are no other side chains with ionizable groups at an acceptable pK_a in the immediate vicinity of the α-carboxylate carbon (Figure 5), the most plausible candidates remaining as general base are the nonbridging phosphate

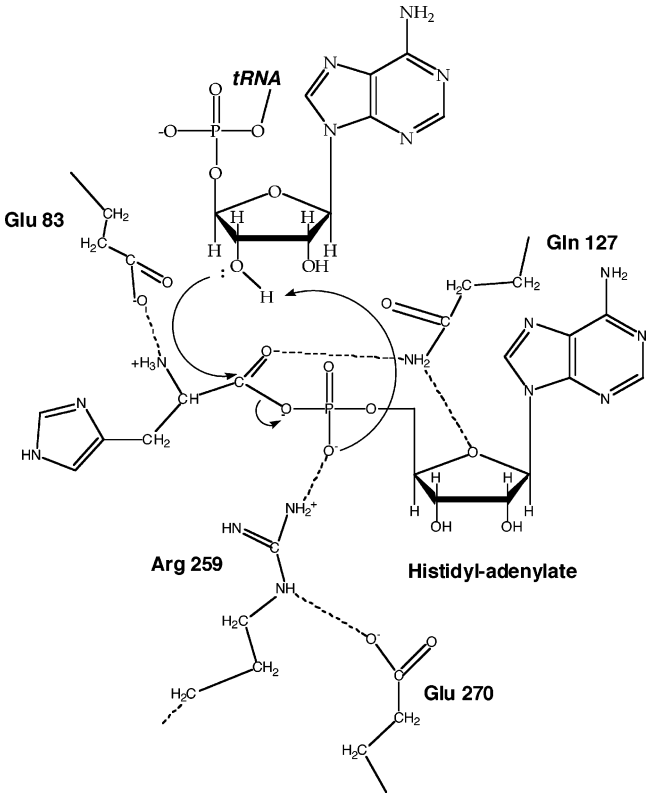

FIGURE 5: Concerted, substrate assisted mechanism for aminoacylation by histidyl−tRNA synthetase.

oxygens of the adenylate. The phosphorothioate experiments reported here constitute the first direct experimental test of this concept, which had been proposed earlier (*17*, *44*). Previous studies employing phosphorothioate substituted substrates indicate that these experiments need to be interpreted carefully (*45*−*47*), both due to the potential for altered geometry and as a consequence of chemical differences related to the P−S bond (*48*). Our comparison of the effects of both diastereomers essentially rules out these trivial explanations and serves to implicate the Sp oxygen as a putative general base. If the basis of the phosphorothioate effect were purely steric, then dramatic decreases in transfer rates for both diastereomers would have ensued, and rescue of the Sp phosphorothioate adenylate by the R259H substitution might well have been observed, by analogy to other systems (*45*, *49*). Although the Rp and Sp oxygens of the adenylate are both in contact with arginines (Arg 113 and Arg259, respectively), the latter interaction is chemically distinct: the ϵ nitrogen of Arg259 makes a salt bridge with Glu270 in the adenylate complex. Consequently, the Arg259-pro-*S* oxygen interaction is likely to be weakened in the adenylate complex, relative to that made by Arg113, facilitating protonation of the pro-*S* oxygen.

A conserved arginine in motif 2 makes a universal contact to the pro-*R* nonbridging oxygen in all class II enzymes, while contacts to the pro-*S* oxygen are idiosyncratic to different families (*5*). Many class II enzymes employ a coordinated magnesium ion for this interaction, while HisRS is unique in making this contact with an arginine. PheRS likely employs a catalytic Mg2+ for contacting the pro-*S* oxygen, yet exhibits the same stereospecificity with respect to utilization of the Rp and Sp isomers of ATPαS as HisRS (*50*). Therefore, the thio stereospecificity we observe is not dependent on the unique Arg259 of HisRS. The generality of this observation is therefore an interesting question to be pursued in other systems; the absence of an appropriately positioned general base in both class I and class II enzymes certainly raises the possibility of generalized substrate assisted catalysis in many aaRSs.

Is a Concerted Transition State General for Aminoacyl−tRNA Synthetases? In classical enzymology, information about transition state structure is obtained from kinetic isotope effects or measurement of Brønsted linear free energy relationships. The high specificity of aaRSs for their substrates prevents systematic leaving group modification, and kinetic isotope effect experiments would be complicated by the solvent exchangeable nature of the key protons. With the caveat that our argument relies on the results of mutagenesis experiments, we find a dissociative transition state for aminoacyl transfer unlikely, as it would require formation of a carbocation at the α-carboxylate carbon and a negatively charged AMP leaving group. In the absence of side chains to stabilize these charged intermediates, this would be thermodynamically unfavorable. A dissociative transition state would further require buildup of charge on the bridging oxygen axial to the phosphate group, one of the few polar groups in the histidinyl adenylate not contacted by HisRS. Chemical activation of the nucleophile, an event of importance in HisRS, should not significantly affect the rate in a dissociative mechanism. Hence, a dissociative mechanism can be ruled out for HisRS.

An associative mechanism for aminoacyl transfer was initially proposed by Perona et al. (*17*) and endorsed by others (*18*, *51*). This mechanism entails formation of a stable tetrahedral intermediate that, by analogy with serine proteases, would include contacts to neutralize the oxyanion. In HisRS, the carboxyamide group of Gln127 contacts the α-carboxylate oxygen, an interaction that does not appear to make a significant contribution to the transition state for aminoacyl transfer (Table 2). Accordingly, we favor a concerted mechanism for aminoacyl transfer (Figure 5), as it provides a better explanation for the key observations reported here. In this mechanism, bond formation between the 3′OH and α-carboxylate carbon would be concerted with the cleavage of the bond joining the α-carboxylate carbon to the axial oxygen of the α-phosphate, thereby rationalizing the considerable pK_a difference between the 3′OH of tRNA (pK_a = 16) and the nonbridging sp oxygen (pK_a = −1). As the bond between the tRNA nucleophile and the α-carboxylate is formed, the pK_a of the 3′OH proton would be expected to drop sharply, while the pK_a of the nonbridging oxygen would tend to rise as the bond to the α-carboxylate begins to lengthen and break. Thus, a concerted mechanism provides a means to enhance the substrate assisted nature of catalysis in this reaction. More recently, it has been proposed that peptidyl transfer by the ribosome is substrate assisted and features the enhancement of catalysis by the P-site tRNA (*52*−*54*). Should such mechanisms be verified for both the aaRS and the ribosome, it would suggest that acid−base catalysis of these fundamental reactions is largely provided by the substrates and that the major role of the aaRS and ribosome is to guide their respective substrates into position for catalysis (*55*).

ACKNOWLEDGMENT

We thank Dr. Fritz Eckstein for the generous gift of ADPαS (Rp), Dr. John Perona for assistance in the development of the rapid quench assay, and Drs. Dieter Söll and John Burke for their comments on the manuscript.

REFERENCES

1. Pauling, L. (1958) *The probability of errors in the process of synthesis of protein molecules*, Birkhauser Verlag, Basel.
2. Martinis, S. A., Plateau, P., Cavarelli, J., and Florentz, C. (1999) Aminoacyl-tRNA synthetases: A family of expanding functions, *EMBO J. 18*, 4591−4596.
3. Ibba, M., and Soll, D. (2000) Aminoacyl-tRNA synthesis, *Annu. Rev. Biochem. 69*, 617−650.
4. Francklyn, C., Perona, J. J., Puetz, J., and Hou, Y. M. (2002) Aminoacyl-tRNA synthetases: versatile players in the changing theater of translation, *RNA 8*, 1363−1372.
5. Arnez, J. G., and Moras, D. (1997) Structural and functional considerations of the aminoacylation reaction, *Trends Biochem. Sci. 22*, 211−216.
6. Leatherbarrow, R. J., Fersht, A. R., and Winter, G. (1985) Transition-state stabilization in the mechanism of tyrosyl-tRNA synthetase revealed by protein engineering, *Proc. Natl. Acad. Sci. U.S.A. 82*, 7840−7844.
7. Fersht, A. R. (1987) Dissection of the structure and activity of the tyrosyl-tRNA synthetase by site-directed mutagenesis, *Biochemistry 26*, 8031−8037.
8. Fersht, A. R. (1988) Relationships between apparent binding energies measured in site-directed mutagenesis experiments and energetics of binding and catalysis, *Biochemistry 27*, 1577−1580.
9. Leatherbarrow, R. J., and Fersht, A. R. (1987) Investigation of transition-state stabilization by residues histidine-45 and threonine-40 in the tyrosyl-tRNA synthetase, *Biochemistry 26*, 8524−8528.
10. Ebel, J. P., Giegé, R., Bonnet, J., Kern, D., Befort, N., Bollack, C., Fasiolo, F., Gangloff, J., and Dirheimer, G. (1973) Factors determining the specificity of the tRNA aminoacylation reaction. Nonabsolute specificity of tRNA-aminoacyl-tRNA synthetase recognition and particular importance of the maximal velocity, *Biochimie 55*, 547−557.
11. Krauss, G., Riesner, D., and Maass, G. (1976) Mechanism of Discrimination between Cognate and Noncognate tRNAs by Phenylalanyl-tRNA Synthetase from Yeast, *Eur. J. Biochem. 68*, 81−93.
12. Dibbelt, L., Pachmann, U., and Zachau, H. G. (1980) Serine activation is the rate-limiting step of tRNASer aminoacylation by yeast seryl tRNA synthetase, *Nucleic Acids Res. 8*, 4021−4039.
13. Dibbelt, L., and Zachau, H. G. (1981) On the rate-limiting step of yeast tRNAPhe aminoacylation, *FEBS Lett. 129*, 173−176.
14. Eldred, E. W., and Schimmel, P. R. (1972) Investigation of the transfer of amino acid from a transfer ribonucleic acid synthetase-aminoacyl adenylate complex to transfer ribonucleic acid, *Biochemistry 11*, 17−23.
15. Yarus, M., and Berg, P. (1969) Recognition of tRNA by isoleucyl-tRNA synthetase. Effect of substrates on the dynamics of tRNA-enzyme interaction, *J. Mol. Biol. 42*, 171−189.
16. Fersht, A. R., and Kaethner, M. M. (1976) Mechanism of aminoacylation of tRNA. Proof of the aminoacyl adenylate pathway for the isoleucyl- and tyrosyl-tRNA synthetases from *Escherichia coli* K12, *Biochemistry 15*, 818−823.
17. Perona, J. J., Rould, M. A., and Steitz, T. A. (1993) Structural Basis for Transfer RNA Aminoacylation by *Escherichia coli* Glutaminyl-tRNA Synthetase, *Biochemistry 32*, 8758−8771.
18. Cavarelli, J., Eriani, G., Rees, B., Ruff, M., Boeglin, M., Mitschler, A., Martin, F., Gangloff, J., Thierry, J.-C., and Moras, D. (1994) The Active Site of Yeast Aspartyl-tRNA Synthetase: Structural and Functional Aspects of the Aminoacylation Reaction, *EMBO J. 13*, 327−337.
19. Francklyn, C., and Arnez, J. G. (2004) in *Aminoacyl-tRNA Synthetases* (Ibba, M., Francklyn, C., and Cusack, S., Eds.) Landes Publishing, Austin, TX.
20. Arnez, J. G., Harris, D. C., Mitschler, A., Rees, B., Francklyn, C. S., and Moras, D. (1995) Crystal structure of histidyl-tRNA synthetase from *Escherichia coli* complexed with histidyl-adenylate, *EMBO J. 14*, 4143−55.
21. Arnez, J. G., Augustine, J. G., Moras, D., and Francklyn, C. S. (1997) The first step of aminoacylation at the atomic level in histidyl-tRNA synthetase, *Proc. Natl. Acad. Sci. U.S.A. 94*, 7144−9.
22. Åberg, A., Yaremchuk, A., Tukalo, M., Rasmussen, B., and Cusack, S. (1997) Crystal structure analysis of the activation of histidine by *Thermus thermophilus* histidyl-tRNA synthetase, *Biochemistry 36*, 3084−94.
23. Qiu, X., Janson, C. A., Blackburn, M. N., Chhohan, I. K., Hibbs, M., and Abdel-Meguid, S. S. (1999) Cooperative structural dynamics and a novel fidelity mechanism in histidyl-tRNA synthetases, *Biochemistry 38*, 12296−12304.
24. Himeno, H., Hasegawa, T., Ueda, T., Watanabe, K., Miura, K., and Shimizu, M. (1989) Role of the extra G−C pair at the end of the acceptor stem of tRNA(His) in aminoacylation, *Nucleic Acids Res. 17*, 7855−7863.
25. Yan, W., Augustine, J., and Francklyn, C. (1996) A tRNA identity switch mediated by the binding interaction between a tRNA anticodon and the accessory domain of a class II aminoacyl-tRNA synthetase, *Biochemistry 35*, 6559−6568.
26. Yan, W., and Francklyn, C. (1994) Cytosine 73 is a discriminator nucleotide in vivo for histidyl-tRNA in *Escherichia coli*, *J. Biol. Chem. 269*, 10022−10027.
27. Hawko, S. A., and Francklyn, C. S. (2001) Covariation of a specificity-determining structural motif in an aminoacyl-tRNA synthetase and a tRNA identity element, *Biochemistry 40*, 1930−1936.
28. Connolly, S. A., Rosen, A. E., Musier-Forsyth, K., and Francklyn, C. S. (2004) G-1:C73 recognition by an arginine cluster in the active site of *Escherichia coli* histidyl-tRNA synthetase, *Biochemistry 43*, 962−969.
29. Eckstein, F., and Goody, R. S. (1976) Synthesis and properties of diastereoisomers of adenosine 5′-(*O*-1-thiotriphosphate) and adenosine 5′-(*O*-2-thiotriphosphate), *Biochemistry 15*, 1685−1691.
30. Francklyn, C., Adams, J., and Augustine, J. (1998) Catalytic Defects in Mutants of Class II Histidyl-tRNA Synthetase from *Salmonella typhimurium* Previously Linked to Decreased Control of Histidine Biosynthesis Regulation, *J. Mol. Biol. 280*, 847−858.
31. Avis, J. M., Day, A. G., Garcia, G. A., and Fersht, A. R. (1993) Reaction of modified and unmodified $tRNA^{Tyr}$ substrates with tyrosyl-tRNA synthetase (*Bacillus stearothermophilus*), *Biochemistry 32*, 5312−5320.
32. Fersht, A. R., and Jakes, R. (1975) Demonstration of two reaction pathways for the aminoacylation of tRNA. Application of the pulsed quenched flow technique, *Biochemistry 14*, 3350−3356.
33. Sankaranarayanan, R., Dock-Bregeon, A.-C., Romby, P., Caillet, J., Springer, M., Rees, B., Ehresmann, C., Ehresmann, B., and Moras, D. (1999) The structure of threonyl-tRNA synthetase-$tRNA^{Tyr}$ complex enlightens its repressor activity and reveals an essential zinc ion in the active site, *Cell 97*, 371−381.
34. Eiler, S., Dock-Bregeon, A., Moulinier, L., Thierry, J. C., and Moras, D. (1999) Synthesis of aspartyl-tRNA(Asp) in *Escherichia coli*—a snapshot of the second step, *EMBO J. 18*, 6532−6541.
35. Kalousek, F., and Konigsberg, W. H. (1974) Purification and characterization of histidyl transfer ribonucleic acid synthetase of *Escherichia coli*, *Biochemistry 13*, 999−1006.
36. Gruic-Sovulj, I., Landeka, I., Soll, D., and Weygand-Durasevic, I. (2002) tRNA-dependent amino acid discrimination by yeast seryl-tRNA synthetase, *Eur. J. Biochem. 269*, 5271−5279.
37. Dibbelt, L., and Zachau, H. G. (1981) The mechanism of salt-induced stimulation of tRNASer aminoacylation by yeast seryl-tRNA synthetase, *FEBS Lett. 131*, 293−295.
38. Fersht, A. R., Gangloff, J., and Dirheimer, G. (1978) Reaction pathway and rate-determining step in the aminoacylation of tRNAArg catalyzed by the arginyl-tRNA synthetase from yeast, *Biochemistry 17*, 3740−3746.
39. Uter, N. T., and Perona, J. J. (2004) Long-range intramolecular signaling in a tRNA synthetase complex revealed by pre-steady-state kinetics, *Proc. Natl. Acad. Sci. U.S.A. 101*, 14396−14401.
40. Ward, W. H. J., and Fersht, A. R. (1988) Tyrosyl-tRNA synthetase acts as an asymmetric dimer in charging tRNA. A rationale for half-of-the-sites activity, *Biochemistry 27*, 5525−5530.
41. Jakubowski, H., and Goldman, E. (1984) Quantities of individual aminoacyl-tRNA families and their turnover in *Escherichia coli*, *J. Bacteriol. 158*, 769−776.
42. Brenner, M., De Lorenzo, F., and Ames, B. N. (1970) Energy charge and protein synthesis. Control of aminoacyl transfer ribonucleic acid synthetases, *J. Biol. Chem. 245*, 450−452.

43. Elf, J., and Ehrenberg, M. (2005) Near-critical behavior of aminoacyl-tRNA pools in *E. coli* at rate limiting supply of amino acids, *Biophys J. 88*, 132−146.
44. Cavarelli, J., Eriani, G., Rees, B., Ruff, M., Boeglin, M., Mitschler, A., Martin, F., Gangloff, J., Thierry, J. C., and Moras, D. (1994) The active site of yeast aspartyl-tRNA synthetase: structural and functional aspects of the aminoacylation reaction, *EMBO J. 13*, 327−337.
45. Admiraal, S. J., Schneider, B., Meyer, P., Janin, J., Veron, M., Deville-Bonne, D., and Herschlag, D. (1999) Nucleophilic activation by positioning in phosphoryl transfer catalyzed by nucleoside diphosphate kinase, *Biochemistry 38*, 4701−4711.
46. Herschlag, D., Piccirilli, J. A., and Cech, T. R. (1991) Ribozyme-catalyzed and nonenzymatic reactions of phosphate diesters: Rate effects upon substitution of sulfur for a nonbridging phosphoryl oxygen atom, *Biochemistry 30*, 4844−4854.
47. Holtz, K. M., Catrina, I. E., Hengge, A. C., and Kantrowitz, E. R. (2000) Mutation of Arg-166 of alkaline phosphatase alters the thio effect but not the transition state for phosphoryl transfer. Implications for the interpretation of thio effects in reactions of phosphatases, *Biochemistry 39*, 9451−9458.
48. Frey, P. A., and Sammons, R. D. (1985) Bond order and charge localization in nucleoside phosphorothioates, *Science 228*, 541−545.
49. Zhang, Y. L., Hollfelder, F., Gordon, S. J., Chen, L., Keng, Y. F., Wu, L., Herschlag, D., and Zhang, Z. Y. (1999) Impaired transition state complementarity in the hydrolysis of *O*-arylphosphorothioates by protein-tyrosine phosphatases, *Biochemistry 38*, 12111−12123.
50. Connolly, B. A., Von der Haar, F., and Eckstein, F. (1980) Structure of the metal·nucleotide complex in the yeast phenylalanyl transfer ribonucleic acid synthetase reaction as determined with diastereomeric phosphorothioate analogues of ATP, *J. Biol. Chem. 255*, 11301−11307.
51. Xin, Y., Li, W., and First, E. A. (2000) Stabilization of the transition state for the transfer of tyrosine to tRNA(Tyr) by tyrosyl-tRNA synthetase, *J. Mol. Biol. 303*, 299−310.
52. Agmon, I., Auerbach, T., Baram, D., Bartels, H., Bashan, A., Berisio, R., Fucini, P., Hansen, H. A., Harms, J., Kessler, M., Peretz, M., Schluenzen, F., Yonath, A., and Zarivach, R. (2003) On peptide bond formation, translocation, nascent protein progression, and the regulatory properties of ribosomes. Derived on October 20, 2002 at the 28th FEBS Meeting in Istanbul, *Eur. J. Biochem. 270*, 2543−2556.
53. Steitz, T. A., and Moore, P. B. (2003) RNA, the first macromolecular catalyst: the ribosome is a ribozyme, *Trends Biochem. Sci. 28*, 411−418.
54. Weinger, J. S., Parnell, K. M., Dorner, S., Green, R., and Strobel, S. A. (2004) Substrate-assisted catalysis of peptide bond format in by the ribosome, *Nat. Struct. Mol. Biol. 11*, 1101−1106.
55. Sievers, A., Beringer, M., Rodnina, M. V., and Wolfenden, R. (2004) The ribosome as an entropy trap, *Proc. Natl. Acad. Sci. U.S.A. 101*, 7897−7901.
56. Ibba, M., Sever, S., Praetorius-Ibba, M., and Soll, D. (1999) Transfer RNA identity contributes to transition state stabilization during aminoacyl-tRNA synthesis, *Nucleic Acids Res. 27*, 3631−3637.

BI047923H